Proceedings of 9th International Symposium on Fluid-Structure Interactions, Flow-Sound Interactions, Flow-Induced Vibration & Noise
July 8-11, 2018, Toronto, Ontario, Canada

FIV2018-131

PASSIVE SUPPRESSION OF TRANSVERSE GALLOPING USING A NON-LINEAR ENERGY SINK

Bianca Teixeira
Offshore Mechanics Laboratory
Escola Politécnica
University of São Paulo, Brazil
Brazil
txrbianca@gmail.com

Guilherme Rosa Franzini
Offshore Mechanics Laboratory
Escola Politécnica
University of São Paulo, Brazil
Brazil
gfranzini@usp.br

Frédérick P. Gosselin
Department of Mechanical Engineering
École Polytechnique de Montréal
Québec, QC
Canada
frederick.gosselin@polymtl.com

ABSTRACT

Flow-induced vibrations (FIV) usually involve self-excited oscillations that can decrease the structural lifespan of engineering structures. For this reason, mitigation or suppression of FIV is of the utmost importance. We use of an absorber named non-linear energy sink (NES) aiming at suppressing vibrations caused by the galloping phenomenon. The NES consists of a rigid rod, free to rotate around the axis of a square prism and with a tip-mass. A linear dashpot connects the NES to the main structure. The equations of motion of the system are non-linear due to both the rotative character of the absorber and the quasi-static hypothesis used in the modeling. The two degrees-of-freedom system composed by the NES and the main structure is investigated in a reduced-order approach. The aerodynamic loads are modeled by using the standard quasi-static approach. We highlight the influence of the parameters that define the rotative absorber such as its radius and damping constant on the response to the galloping excitation. We show that the NES can significantly reduce the galloping response.

NOMENCLATURE

M Prism mass *per* unit length
k Stiffness
c Damping constant
D Prism side
Y Prism displacement
m Suppressor mass *per* unit length
r Suppressor *radius*
θ Suppressor displacement
c_θ Suppressor damping
ρ Fluid density
U_∞ Free-stream velocity

INTRODUCTION

Flow-induced vibrations (FIV) phenomena usually involve self-excited oscillations. Examples of FIV phenomena are vortex-induced vibrations (VIV), flutter and galloping, the latter being the focus of this paper. Further details about FIV can be found in the comprehensive textbooks [1], [2] and [3].

Galloping is a type of dynamic instability, occurring when the total damping (i.e., the sum of the structural damping with that provided by the aerodynamic load)

is negative. A technological importance of this phenomenon is on the dynamics of power-lines covered by ice. Contrary to VIV, the oscillation amplitudes increases with the increasing in the free-stream velocity. Hence, it is of practical importance to study manners on suppressing galloping.

Recently, a class of passive suppressors named nonlinear energy sinks (NES) has received a series of efforts. Following the comphrensive literature review [4], a NES generally requires a damper (usually, a linear one) and a non-linearizable natural frequency, responsible for enabling the suppressor to responds for a different types of excitation. The motion of the main structure induces the NES to respond. Part of the kinetic energy of the NES is locally dissipated on its damper, defining a process named Targeted Energy Transfer (TET). Further discussions regarding NES and TET can be found, for example, in the references [5] and [6].

There is a large number of recent contributions focusing on the passive suppression of VIV using NES - see [7], [8], [9], [10], [11] and [12]. Luongo and Zulli ([13]) studied the dynamics of a two degrees-of-freedom foil subjected to an uniform free-stream velocity. By using a mixed multiple scale/harmonic balance method, the authors pointed out that a NES can be used to increase the critical velocity for the aeroelastic instability and to decrease the post-critical oscillation amplitudes.

In the recent work [14], the authors employed a translational NES as a passive suppressor of galloping of a one degree-of-freedom square prism. The translational NES consisted of a small mass, constrained to oscillate in the same direction of the prism and coupled to it by means of a non-linear spring and a linear damper. Among other results, this reference points out the capacity of the NES to reduce the galloping oscillations.

The present paper aims at contributing with passive suppression of galloping. Contrary to [14], a rotational NES is used to control the oscillations of a square prism subjected to galloping.

MATHEMATICAL MODEL

In this paper, we develop a bidimensional modeling of the problem. Consider a square prism of side D and mass *per* unit length M assembled into an elastic base defined by its stiffness k and linear damping constant c, both *per* unit length. The prism is constrained to oscillate only in the cross-wise direction. The fluid has density ρ and the free-stream velocity is supposed to be constant and equal to U_∞. The rotative NES consists of a rigid rod of length r and mass *per* unit length m. The NES is connected to the prism by means of a linear dashpot of constant c_θ. Fig. 1 sketches the problem.

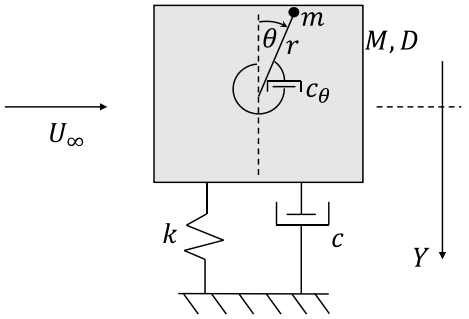

FIGURE 1: SCHEMATIC REPRESENTATION.

The equations of motion are obtained in the dimensional form by using the Euler-Lagrange's equation. Further details regarding analytical mechanics equation can be found, for example, in [15]. For the sake of conciseness, the derivation is not presented. Eqs. 1 and 2 present the dimensional form of the equations of motion.

$$(M+m)\frac{d^2Y}{dt^2} + mr\left[\sin\theta\frac{d^2\theta}{dt^2} + \cos\theta\left(\frac{d\theta}{dt}\right)^2\right] + \\ + c\frac{dY}{dt} + kY = \frac{1}{2}\rho U_\infty^2 D C_y \tag{1}$$

$$mr^2\frac{d^2\theta}{dt^2} + mr\sin\theta\frac{d^2Y}{dt^2} + c_\theta\frac{d\theta}{dt} = 0 \tag{2}$$

In Eqs. 1 and 2, the aerodynamic load is *per* unit length. The aerodynamic force coefficient in the cross-wise direction C_y is calculated using the *quasi*-static approach using Eq. 3. Such a hypothesis is valid if the vortex-shedding frequency is much higher than the natural frequency of the system.

$$C_y = \sum_{k=1}^{N} a_k \left(\frac{\frac{dY}{dt}}{U_\infty} \right)^k \tag{3}$$

Aiming at achieving a more general aspect, the equations of motion are now rewritten in the dimensionless form. For this, consider the following dimensionless quantities:

$$y = \frac{Y}{D}, \hat{r} = \frac{r}{D}, \tau = t\omega = t\sqrt{\frac{k}{M+m}}, \zeta_y = \frac{c}{2(M+m)\omega}$$
$$\zeta_\theta = \frac{c_\theta}{2mr^2\omega}, U_r = \frac{U_\infty}{\omega D}, \hat{m} = \frac{m}{M}, m^* = \frac{M+m}{\rho D^2} \tag{4}$$

Introducing the quantities given by Eq. 4 in Eqs. 1 and 2, the dimensionless equations of motion are given by Eqs. 5 and 6.

$$\ddot{y} + \frac{\hat{m}}{1+\hat{m}}\hat{r}(\sin\theta\ddot{\theta} + \cos\theta\dot{\theta}^2) + 2\zeta_y\dot{y} + y =$$
$$= \frac{U_r^2}{2m^*}\left[a_1\left(\frac{\dot{y}}{U_r}\right) + a_2\left(\frac{\dot{y}}{U_r}\right)^2 + a_3\left(\frac{\dot{y}}{U_r}\right)^3 \right] \tag{5}$$

$$\ddot{\theta} + \frac{1}{\hat{r}}\sin\theta\ddot{y} + 2\zeta_\theta\dot{\theta} = 0 \tag{6}$$

being $(\dot{})$ the derivative with respect to τ.

ANALYSIS METHODOLOGIES

Firstly, we present the methodology employed for the numerical simulations. Eqs. 5 and 6 are numerically integrated using the Runge-Kutta scheme. The adopted time-step is $\Delta\tau = 0.01$ and the simulations last $\tau_{max} = 800$. The initial conditions are $y(0) = 0.10$, $\theta(0) = \pi/6$ and $\dot{y}(0) = \dot{\theta}(0) = 0$. The characteristic oscillation amplitude $\hat{A}$ is obtained by taking the maximum value of $y(\tau > \tau_{max}/2)$. Such a procedure aims at avoiding transient responses. According to [3], the following aerodynamic coefficients are adopted for a square section: $a_1 = 2.69$, $a_2 = 0$ and $a_3 = -168.4$.

As this paper focuses on the influence of the different NES parameters on the suppression, two simulations groups are discussed. In Group 1, we study the effects of changing the NES *radius*. In Group 2, different NES damping ratios ζ_θ are simulated. Tab. 1 presents the simulations groups. The mass of the suppressor corresponds to $\hat{m} = 0.10$ for all simulations.

TABLE 1: SIMULATION GROUPS.

Group 1 $\zeta_\theta = 0.05$		Group 2 $\hat{r} = 0.30$	
Sim	$\hat{r}$	Sim	ζ_θ
G1-Sim1	0.10	G2-Sim1	0.05
G1-Sim2	0.20	G2-Sim2	0.08
G1-Sim3	0.30	G2-Sim3	0.10
G1-Sim4	0.40	G2-Sim4	0.12
G1-Sim5	0.50	G2-Sim5	0.15

Throughout this paper, the mass parameter is $m^* = 393$, in agreement with the experimental setup that is being tested at the wind tunnel facility existent at École Polytechnique de Montréal (PolyMTL). The structural damping ratio is also invariant and equal to $\zeta_y = 0.01$.

RESULTS AND DISCUSSION

Fig. 2 presents the variation of $\hat{A}$ with the reduced velocity U_r for the simulations pertaining to Group 1. This figure reveals two interesting aspects, the first one being related to the critical reduced velocity for the galloping. Notice that the presence of the suppressor does not have significant impact on the onset of the self-excited oscillations. On the other hand, the suppressor has a marked influence on the post-critical response. The characteristic oscillation amplitude for the pure galloping (i.e, without the NES) has an upward trend with the reduced velocity. In turn, the presence of the NES decreases the prism oscillation in the interval $6.5 < U_r < 12$. Such a decrease is significant and sometimes the oscillation amplitude of the prism with NES is half that observed without the suppressor. In addition, one clearly notices that the case with the small *radius*, G1-Sim1, is the more efficient condition

tested in Group 1 for reduced velocities up to $U_r = 12$. Beyond this value, the oscillation amplitudes are the same observed for pure galloping.

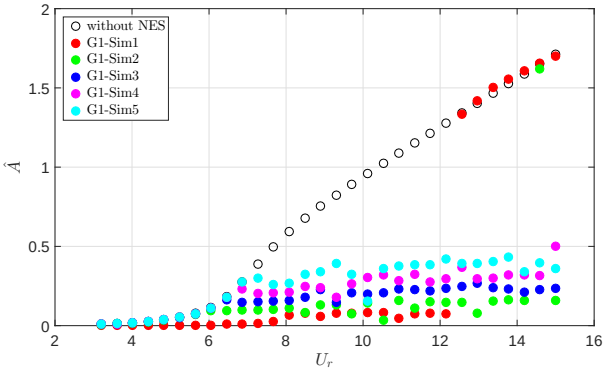

FIGURE 2: OSCILLATION AMPLITUDE AS A FUNCTION OF THE REDUCED VELOCITY - GROUP 1.

Assessments of the NES damping are made in Figs. 3 and 4. Surprisingly, variations in ζ_θ do not significantly change the prism oscillation of response, even for the suppressor with $\hat{r} = 0.10$, the most effective suppression scenario.

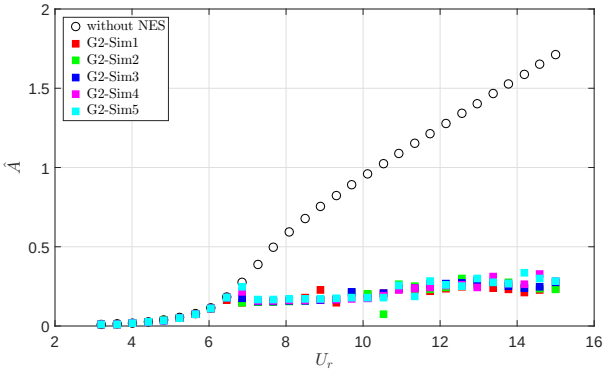

FIGURE 3: OSCILLATION AMPLITUDE AS A FUNCTION OF THE REDUCED VELOCITY - GROUP 1.

Quantitative aspects of the response are now explored. For the sake of limitation of the paper length, only one example is herein discussed. Fig. 5 presents the prism response and the corresponding amplitude spectra obtained at $U_r = 10.93$. Consider, firstly, the simulation without NES (see Fig. 5(a)), a steady-state regime of amplitude $\hat{A} = 1.07$ is reached for $\tau > 400$. As expected, the prism oscillates with its natural frequency (i.e, $\hat{\omega} = 1$).

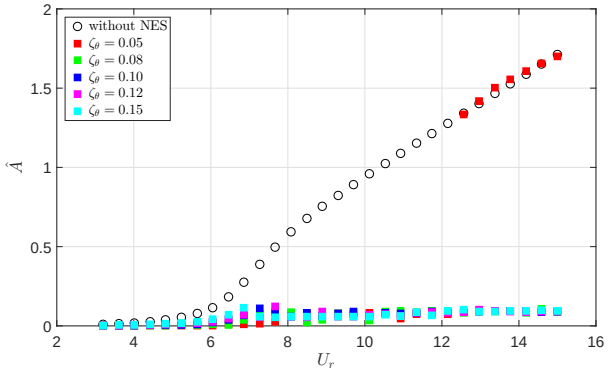

FIGURE 4: OSCILLATION AMPLITUDE AS A FUNCTION OF THE REDUCED VELOCITY. $\hat{r} = 0.10$.

Consider now the prism response for the case G1-Sim3 presented in Fig. 5(b). Contrary to the pure galloping, the response of the prism fitted with this suppressor does not reach a steady-state. Furthermore, the time-history $y(\tau)$ is characterized by intermittent and repetitive cycles of growing and suppression, similarly to what was found in [16] for the passive suppression of parametric instability using a rotative NES. Even though the non-stationary response, the maximum prism displacement is significantly lower than that observed for the pure galloping case.

Now, we investigate the NES response shown in Fig. 6(a). Notice that during the growing regime of the prism response, the NES is characterized by a constant angular position. Furthermore, such an angular position gives $\cos\theta = 1$ (see Fig. 6(b)), corresponding to the NES aligned with the direction of the prism oscillation after some complete rotations. The mathematical explanation for the growing regime is similar to that discussed in [17]. In this regime $\dot{\theta} \approx 0$ and $\cos\theta \approx 1$ (and, consequently, $\sin\theta \approx 0$). Taking these results to Eq. 5, the standard galloping equation is obtained.

The dimensionless angular velocity $\dot{\theta}(\tau)$ is presented in Fig. 6(c). As expected, during the growing regime, $\dot{\theta} = 0$. On the other hand, its behavior during the suppression regime is more complicated. Even though Fig. 6(a) suggests a practically constant angular velocity, the time-history $\dot{\theta}(\tau)$ presents modulations. Furthermore, notice that during the three suppression cycles presented, a clear trend in the angular acceleration $\ddot{\theta}(\tau)$ can be noticed. Such a trend is, in absolute value, equal for the three cy-

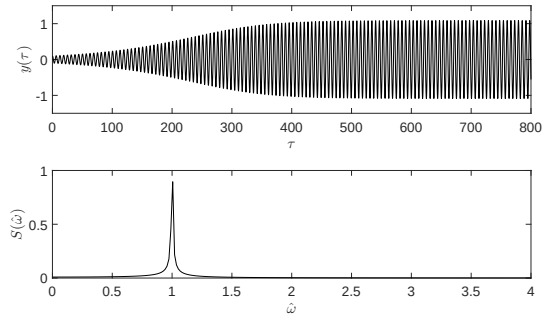

(a) Without NES.

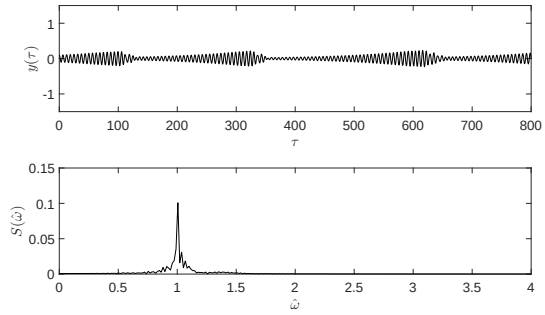

(b) G1-Sim3.

FIGURE 5: EXAMPLES OF PRISM RESPONSE. $U_r = 10.93$.

cles. Curiously, the behavior of the angular response is distinct from that exemplified in [12] for the dynamics of a cylinder fitted with a rotative NES and subjected to VIV. In the example showed in the latter paper, the NES responds with a constant angular velocity.

CONCLUSION

This paper numerically addressed passive suppression of the galloping phenomenon on a square prism. In fact, this is the first of a series of ongoing works on the theme at both Offshore Mechanics Laboratory, Escola Politécnica (LMO) and École Polytechnique de Montréal (PolyMTL). The dimensionless equations of motion of the two degrees-of-freedom system were numerically integrated. The aerodynamic loads were modeled using the *quasi*-static approach. A rotative non-linear energy sink (NES) was employed as the passive suppressor.

In the simulations herein discussed, the mass of the NES was kept constant and equal to 10% of the mass of the prism. The influence of the *radius* and the damping of the NES were assessed. As a major finding of this paper, we highlight the effectiveness of the NES on suppressing

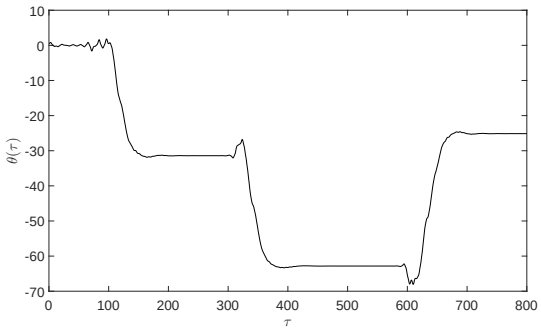

(a) Entire simulation.

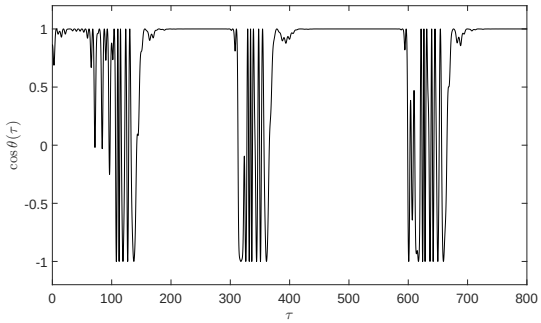

(b) $\cos\theta$.

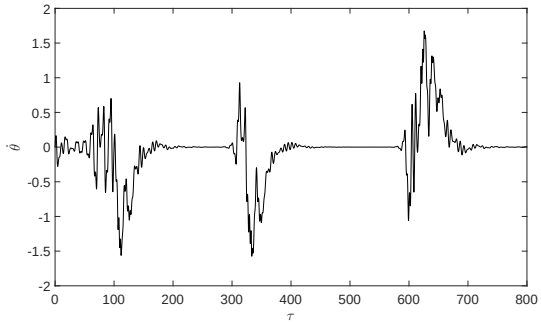

(c) Angular velocity $\dot{\theta}(\tau)$.

FIGURE 6: EXAMPLE OF NES RESPONSE - G1-Sim3. $U_r = 10.93$.

the galloping. Depending on the reduced velocity (i.e, the free-stream velocity normalized with respect to the the natural frequency and the cross-section dimension), the maximum prism response can by less than half that observed without the NES.

For the sake of limitation on the paper length, only one example of response was investigated. Contrary to the case without the NES, the response of the system composed of the prism and the suppressor is non-stationary and characterized by two distinct and intermittent regimes. In the growing regime, the prism amplitude is increased while the NES practically did not respond.

On the suppression regime, the NES rotated and consequently, dissipated energy at its dashpot.

Ongoing works include both experiments being carried out at the PolyMTL wind tunnel facility. In addition to the experimental-numerical correlation, deeplier numerical studies on the influence of the NES parameters are also planned.

ACKNOWLEDGEMENTS

From December, 2017 to February, 2018, the second author developed research activities at École Polytechnique de Montréal with financial support from Fond de Recherche du Québec. The second author is also grateful to the Brazilian National Council of Research (CNPq) for the grant 310595/2015-0. São Paulo Research Foundation (FAPESP) is acknowledged for sponsoring a research project on passive suppression of oscillations using NES, grant 2016/20929-2.

REFERENCES

[1] Blevins, R., 2001. *Flow-Induced Vibration*. Krieger.

[2] Naudascher, E., and Rockwell, D., 2005. *Flow-Induced Vibrations - an engineering guide*. Dover.

[3] Païdoussis, M. P., Price, S. J., and de Langre, E., 2011. *Fluid-Structure Interactions - Cross-Flow-Induced Instabilities*. Cambridge University Press.

[4] Lee, Y. S., Vakakis, A. F., Bergman, L. A., McFarland, D. M., Kerschen, G., Nucera, F., Tsakirtzis, S., and Panagopoulos, P. N., 2008. "Passive non-linear targeted energy transfer and its applications to vibration absorption: a review". *Journal of Multi-body Dynamics,* ***222***(77-134).

[5] Gendelman, O. V., Manevitch, L. I., Vakakis, A. F., and MCloskey, R., 2001. "Energy pumping in nonlinear mechanical oscillators: Part I-dynamics of the underlying hamiltonian systems". *Journal of Applied Mechanics,* ***68***(1), pp. 34–41.

[6] Vakakis, A. F., and Gendelman, O. V., 2001. "Energy pumping in nonlinear mechanical oscillators: Part II - resonance capture". *Journal of Applied Mechanics,* ***68***(1), pp. 42–48.

[7] Tumkur, R. K. R., Calderer, R., Masud, A., Pearlstein, A. J., Bergman, L. A., and Vakakis, A. F., 2013. "Computational study of vortex-induced vibration of a sprung rigid cylinder with a strongly nonlinear internal attachment". *Journal of Fluids and Structures,* ***40***, pp. 214–232.

[8] Tumkur, R. K. R., Domany, E., Gendelman, O. V., Masud, A., Bergman, L. A., and Vakakis, A. F., 2013. "Reduced-order model for laminar vortex-induced vibration of a rigid circular cylinder with an internal nonlinear absorber". *Communications in Nonlinear Science and Numerical Simulation,* ***17***, pp. 1916–1930.

[9] Blanchard, A. B., Gendelman, O. V., Bergman, L. A., and Vakakis, A. F., 2016. "Capture into a slow-invariant-manifold in the fluid-structure dynamics of a sprung cylinder with a nonlinear rotator". *Journal of Fluids and Structures,* ***63***, pp. 155–173.

[10] Tumkur, R. K. R., Pearlstein, A. J., Masud, A., Gendelman, O. V., Blanchard, A. B., Bergman, L. A., and Vakakis, A. F., 2017. "Effect of an internal nonlinear rotational dissipative element on vortex shedding and vortex-induced vibration of a sprung circular cylinder". *Journal of Fluid Mechanics,* ***828***, pp. 196–235.

[11] Dai, H. L., Abdelkefi, A., and Wang, L., 2017. "Vortex-induced vibrations mitigation through a nonlinear energy sink". *Communications in Nonlinear Science and Numerical Simulation,* ***42***, pp. 22–36.

[12] Ueno, T., Sato, B. S., and Franzini, G. R., 2018. "A numerical study of VIV suppression using a rotative NVA (non-linear vibration absorber) and a wake-oscillator model". In Proceedings of the 9th International Symposium on Fluid-Structure Interactions, Flow-Sound Interactions, Flow-Induced Vibration & Noise (submitted).

[13] Luongo, A., and Zulli, D., 2014. "Aeroelastic instability analysis of NES-controlled systems via a mixed multiple scale/harmonic balance method". *Journal of Vibration and Control,* ***20(13)***, pp. 1985–1998.

[14] Dai, H. L., Abdelkefi, A., and Wang, L., 2016. "Usefulness of passive non-linear energy sinks in controlling galloping vibrations". *International Journal of Non-Linear Mechanics,* ***81***, pp. 83–94.

[15] Meirovitch, L., 2003. *Methods of Analytical Dynamics*. Dover Publications.

[16] Campedelli, G. R., Franzini, G. R., and Mazzilli, C. E. N., 2018. "Further numerical studies on passive

suppression of parametric instability using a rotative non-linear energy sink". In Proceedings of the IUTAM Symposium "Exploiting Nonlinear Dynamics for Engineering Systems' - ENOLIDES (submitted).

[17] Franzini, G. R., Campedelli, G. R., and Mazzilli, C. E. N. "A numerical investigation on passive suppression of the parametric instability phenomenon using a rotative non-linear vibration absorber". *International Journal of Non-Linear Mechanics (submitted)*.